Data-Driven Simulation of the Rockmass Response to Mining (Part 2)—Numerical Modelling of the "Room and Pillar" Experiment

R.J. Durrheim Division of Mining Technology, CSIR, South Africa
D. Labrie Mining and Mineral Sciences Laboratories, CANMET, Natural Resources Canada

Many mining excavations are situated in overstressed regimes where the rock surrounding any void will fracture and fail, regardless of the rock-breaking method or shape of the excavation. Numerical modelling tools are widely used to determine which mining geometries and sequences will limit the extent of rock failure and to establish the optimum trade-off between the rock engineering ideal and various economic and practical considerations. This study seeks to advance efforts to simulate the deformation and failure of the Rockmass during mining by integrating physical observations in the numerical modelling process. A simple "room and pillar" model was carved from a 25 cm sandstone cube and loaded triaxially until failure. Comprehensive data sets were gathered for use in the calibration, evaluation and improvement of numerical modelling codes. This paper reviews the sustained efforts of researchers working in the deep gold mines of South Africa and the Underground Research Laboratory in Canada to couple theoretical, laboratory and underground studies with numerical modelling. Key issues in the implementation of data-driven modelling scheme are discussed, and the testing of several CANMET-MMSL numerical modelling codes (Rock^{3D}FE, CANSAFE^{3D} and BSM^{3D}) is described and opportunities for improvement identified.

1 INTRODUCTION

Some operating mines and many prospects are situated in stress regimes where the rock surrounding any void will fracture and fail, regardless of the rock-breaking method or the shape of the excavation (Durrheim, 2002; Udd, 2002). The task of the rock engineer is to design the geometry and sequence of excavations so that the risk of rock failure is limited, and to design functional and cost-effective support systems that will control the fractured rock surrounding the excavations (Wagner, 1989). Numerical modelling tools are generally used to evaluate a range of possible mine designs to find the optimum trade-off between the rock engineering ideal and various economic and practical considerations.

In a recent review of the "state of the art" of numerical modelling, Jing (2003) notes that the *"discontinuous, inhomogeneous, anisotropic and not-elastic"* nature of many Rockmasses makes reliable simulation exceptionally difficult. Jing (2003) concludes: *"our confidence in the numerical models can be raised when they are successfully calibrated against well-controlled laboratory and* in situ *experiments, and when their output for analysing practical problems follows both the basic laws of physics and engineering experience."* This concisely describes the contribution we hope to make with this study.

Laboratory experiments make it possible to evaluate new modelling concepts and monitoring technologies relatively quickly and cost-effectively, as the physical properties of the model can be comprehensively determined, the applied stresses can be precisely controlled, and the deformation adequately measured. While our laboratory models are analogous to mining situations, we have not attempted to create scale models. Our goal is to gather observational data that can be used to calibrate, evaluate and improve existing numerical modelling codes.

The objectives of this study are extremely practical. We aim to develop techniques to incorporate field measurements into numerical modelling codes, thereby improving the match between modelling and reality. We then intend to formulate guidelines that will enable mine operators to apply their data-gathering resources in the most cost-effective way. For example, to decide how best to direct resources between exploration drilling, geotechnical mapping, laboratory rock testing, in situ stress measurements and monitoring instrumentation such as microseismic systems and strain cells. This will assist the designers and operators of mines excavated in overstressed rock to reduce the risk of rockfalls and rockbursts. Furthermore, this work has the potential to improve the efficiency of mining methods that exploit the controlled failure of rock.

2 SIMULATING THE ROCKMASS RESPONSE TO MINING

2.1 Laboratory Experiments

A simple "room and pillar" model was carved from a 25 cm cube of Nepean sandstone, which is a coarse-grained silica rock with a porosity of about 15 per cent. The rock engineering properties were determined by uniaxial, triaxial and diametral tests on a core drilled from the centre of the cube. Durrheim and Labrie (2004) describe the laboratory experiments performed to gather the basic data used for the numerical modelling exercise. Sensors and cameras were used to monitor the deformation, acoustic emission and the evolution of damage. The blocks were sliced after completing the tests and the fractures were mapped. The stress-strain curves are shown in Figure 1 and the parameters listed in Table 1.

Brady and Brown (1985) summarize the principal modes of pillar deformation and failure:

- *Spalling from the pillar surface* is the dominant pillar rupture mode in relatively massive rock, producing necking of the pillar. Pillars with a low height/width ratio in massive rock almost invariably fail in this manner.
- *Inclined shear fractures* may form in pillars with a high height/width ratio, or in pillars that are intersected by transgressive fractures whose angle of inclination exceeds their effective angle of friction.

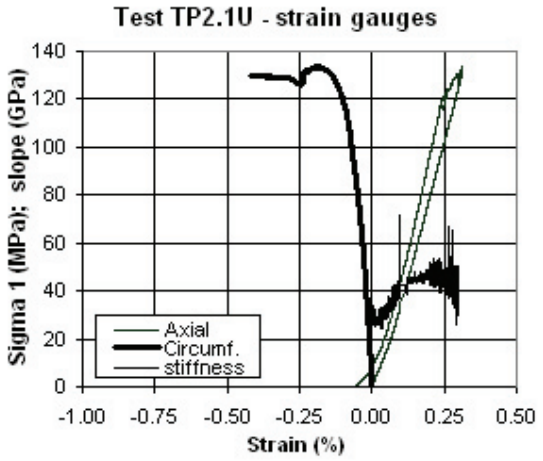

(a)

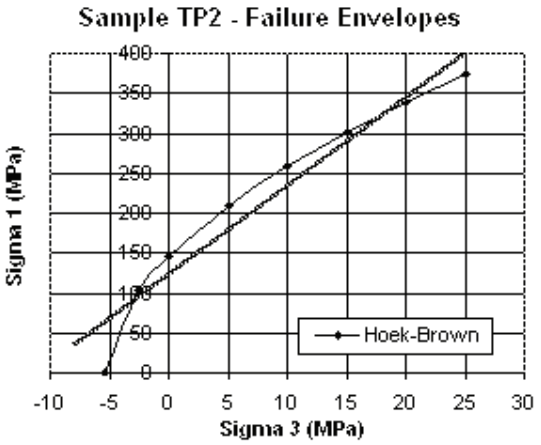

(b)

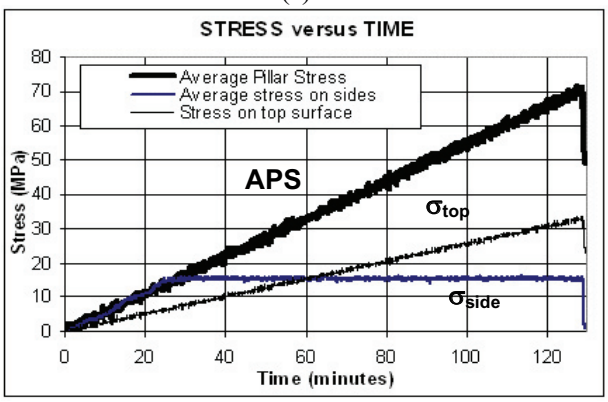

(c)

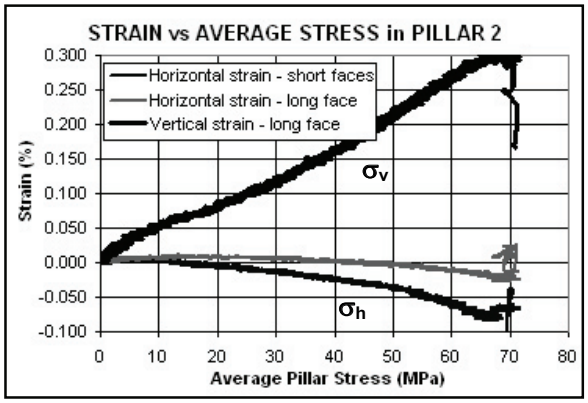

(d)

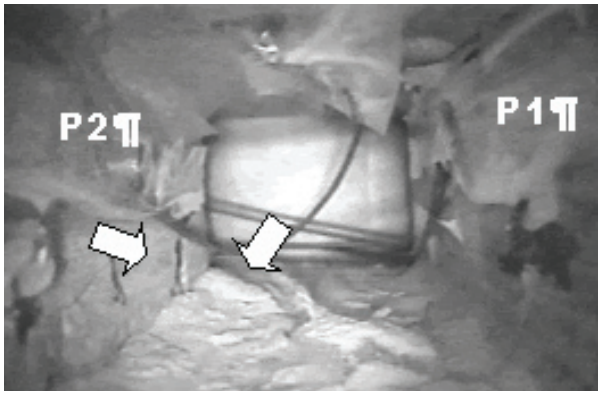

(e)

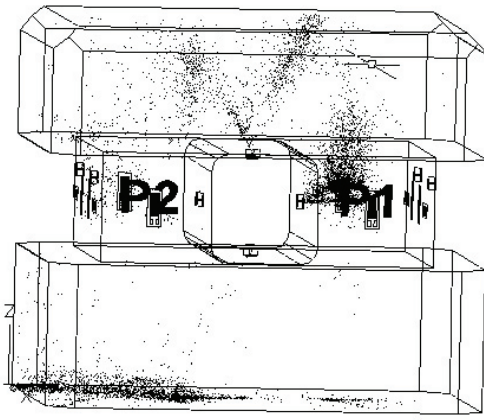

(f)

FIG. 1 **Block #2 tests and experiment (a) Uniaxial test, the axial stiffness was determined by a moving-point regression of the stress-strain curve (b) Hoek-Brown and Mohr-Coulomb failure envelopes (c) Loading of block (d) Deformation of Pillar 2 (e) Video image at the termination of the experiment - note the heave of the floor and slabbing of the Pillar 2 sidewall (f) Acoustic emissions recorded during the experiment - note that the set of source locations is incomplete as two of the eight sensors became detached early in the course of the experiment**

TABLE 1 Properties of Nepean sandstone cube

Uniaxial compressive strength	133.6 MPa
Tensile strength	4.5 MPa
Young's modulus, E	45.2 GPa
Poisson's ratio, υ	0.33
Density	2400 kg/m^3
Hoek-Brown parameters	
σ_c	146.8 MPa
m	27.4
s	1.0
Mohr-Coulomb constants	
σ_c	122.7 MPa
ψ	85°
Cohesion C	18.3 MPa
φ	57°

- *Internal axial splitting* may occur if soft partings are present along the pillar/country rock contact. This failure mode is revealed externally as lateral bulging or barrelling of the pillar surfaces.
- *Buckling failure* may occur if a well-developed foliation or schistosity parallel to the principal axis of loading is present.

An inclined shear fracture formed in Pillar 1, while Pillar 2 failed by spalling from the surface (Figure 2).

2.2 Numerical Modelling

This study draws extensively on the sustained efforts of researchers working in the deep gold mines of South Africa and the Underground Research Laboratory in Canada to couple theoretical, laboratory and underground studies with numerical modelling.

2.2.1 Deep gold mines, South Africa

The challenges of mining at depths approaching 4 km in the Witwatersrand Basin of South Africa has provided the motivation for studies of the brittle failure of rock that range in scale from the sub-millimetre dimensions of mineral grains to gold mines that exceed 20 square kilometres in area.

Fracture and damage mechanics

In a pioneering microfractographic examination of argillaceous quartzite cylinders subjected to triaxial compression, Hallbauer et al. (1973) concluded that most microcracks were initiated by the point loading of quartz grains by other grains with a different crystallographic orientation or another favourably oriented hard mineral (e.g. pyrite, zircon). Micaceous material between grains inhibited microcrack formation. The length of the microcracks was determined largely by the grain size; the crack density was found to be largely dependent on the relative stress level; and the vast majority of microcracks were orientated within 10° of the direction of maximum compressive stress.

Gay (1976) monitored the deformation of quartzite blocks containing holes of varying shapes and sizes subjected to uni- and biaxial compression. The blocks were about 100x100x75 mm^3 in size, and the holes typically 25 mm long and 2 to 5 mm wide. In a series of "mining tests", the holes were enlarged while the samples were under load. Fracture growth was studied by carefully monitoring the surface of the sample while the tests were in progress, and examining polished and thin sections once the tests were completed. It was found that the fractures created in the laboratory resembled those seen in deep mines. These laboratory studies were used some 20 years later to validate an anisotropic damage model implemented in a finite element program that uses the concept of a "sliding flaw" to simulate the microcracking mechanisms characteristic of brittle rock in compression (Sellers and Scheele, 1996). The model successfully described the evolution of damage and the onset of failure.

In another attempt to simulate the stress environment and fracturing around deep level stopes, quartzite specimens were loaded hydrostatically after which the axial stress was reduced until failure occurred (Briggs and Vieler, 1984). The macrofracturing in quartzite produced by these triaxial extension tests was numerically simulated (Malan and Napier, 1995) using the displacement discontinuity boundary element code DIGS (Discontinuity Interaction and Growth Simulation, Napier, 1990), which extends the range of phenomena modelled beyond intergranular fracturing to include intra- and transgranular fracturing. DIGS successfully replicated the observations that the microcracks induced by compressive stress are extensile and sub-parallel to the maximum compressive stress.

Time-dependent behaviour

Discontinuities such as joints, faults, mining-induced fractures and readily mobilized bedding planes penetrate the Rockmass surrounding excavations and enable viscous deformation, with the result that rockbursts may occur hours or even days after blasting. Efforts to simulate time-dependent behaviour measurements made in the laboratory and in the field exemplify the subtle nature of rock creep (see review by Malan, 2002). Malan (1999) implemented a continuum viscoplastic model with a novel time-weakening rule in the FLAC finite difference code. The time-dependant closure of stopes and squeezing conditions in hard rock tunnels were reasonably well simulated. The continuum approach has limitations in situations where the squeezing behaviour is dominated by prominent discontinuities such as bedding planes. The displacement discontinuity technique DIGS was found to yield better results (Napier and Malan, 1997). DIGS assumes that the intact rock material behaves in an essentially elastic manner and that all inelastic behaviour, including viscoplastic effects, is controlled by the presence of multiple interacting discontinuities. It is able to simulate primary, secondary and tertiary creep and the release of seismic energy. DIGS has been validated by comparing its output with measurements of the deformations produced by mining a highly stressed pillar and excavating a tunnel in squeezing rock (Napier and Malan, 1997; Malan, 2002).

Seismicity

There have been concerted efforts to develop methods to integrate the analysis of seismic data with numerical modelling (Spottiswoode, 2001; Hoffman et al., 2001). The MinSInt (Mining and Seismicity Integrator) program compares, in space and time, the observed and the simulated seismicity (Spottiswoode et al., 2003). It has been used to demonstrate that the total amount of seismicity induced by mining is better quantified by the elastic energy change than by the area mined, and that deviations from the elastic model can be explained by the influence of geological features and time-dependant inelastic deformation.

The acoustic emissions produced by microcracking during uniaxial compression of quartzite cylinders were used to investigate the scaling of the rock fracture process (Sellers et al., 2003). The study confirmed that the fracture processes observed in the laboratory are similar to those occurring near stope faces and pillars in deep gold mines where the stress regime is characterized by a vertical stress and low confinement.

2.2.2 Underground Research Laboratory, Canada

The Underground Research Laboratory (URL) of Atomic Energy of Canada Ltd, located within the massive, sparsely

fractured Lac-du-Bonnet granite batholith, has provided the site for a unique series of field, laboratory and numerical modelling studies of brittle rock failure. As part of the Mine-by Experiment (Martin, 1997), a 46 m long, 3.5 m diameter circular test tunnel was excavated without the aid of explosives at a depth of 420 m, approximately parallel to σ_2. The in situ stress magnitudes at the 420 Level are approximately σ_1 = 60 MPa, σ_2 = 45 MPa and σ_3 = 11 MPa, with σ_1 close to horizontal. Lac-du-Bonnet granite has a laboratory unconfined peak strength σ_c of 225 MPa, and a long-term strength σ_{cd} of about $0.7\sigma_c$ or 160 MPa. Displacements, strains, stress changes and acoustic emissions were monitored with state-of-the-art equipment. The geotechnical instrumentation included two triaxial strain cells installed prior to the excavation of the tunnel and a microseismic system.

The primary purpose of the Mine-by Experiment was to investigate brittle failure processes, with findings applicable to mining excavations such as shafts, tunnels and ore passes. Spalling of the rock produced V-shaped notches (or breakouts) on opposite sides of the tunnel in regions of maximum tangential stress (Martin et al., 1997). The notch in the roof stabilized at a depth of 30 to 50 per cent of the tunnel radius, while the development of the notch in the floor was inhibited by the confinement provided by gravity. It was found that crack-induced damage, both in the laboratory and in situ, begins at approximately $\sigma_c/3$, and that the stress level at which failure initiates is affected by the loading path.

Constitutive models

Many constitutive models and numerical modelling codes have been used to back-analyse brittle failure phenomena at the URL, particularly the zone of brittle failure in the Mine-by Experiment test tunnel. These studies, summarized below, amply demonstrate the challenges of modelling Rockmass behaviour even in the simplest of situations.

The two-dimensional elastic boundary element program EXAMINE^{2D} (Curran and Corkum, 1995) was used to simulate the progressive nature of the failure process by manually updating the model to remove material on the tunnel boundary that was indicated to have failed (strength factor < 1 with the Hoek-Brown *s* parameter = 0.25) and repeating the analysis (Martin, 1997). It was found that the depth of failure was overestimated.

ROCK^{3D}FE, a three-dimensional static linear elastic finite element program (Yu et al., 1996 and 1999; Li et al., 2002), was used by Labrie et al. (2002) to model the notch. The Geological Strength Index was used as a basis to reduce the Hoek-Brown *m* and *s* parameters (Hoek and Brown, 1997) and failed elements were removed, but neither the localization of damage or the shape of the notch was successfully simulated.

The various constitutive models that have been implemented in the finite difference code FLAC^{2D} (Itasca, 1995a) are reviewed by Hajiabdolmajid et al. (2002). These include:

- Elastic constitutive model combined with an element removal scheme. The depth of the breakout zone was overestimated by 2- to 3-fold.
- Elastic perfectly-plastic constitutive model. The stress redistribution that occurs when the rock strength is exceeded is simulated. The model ignores material weakening, however, and thus only the minimum depth of failure is given.
- Elastic brittle-plastic constitutive model. The slabbing process is simulated by decreasing the Hoek-Brown m and s parameters to very small values in the post-peak range. As with the elastic-perfectly plastic model, the depth of failure is underestimated and the lateral extent of failure overestimated.
- Cohesion-weakening frictional-strengthening (CWFS) constitutive model. This model incorporates the strains at which residual cohesion and frictional strength are mobilized and successfully modelled the extent of the breakout zone in the Mine-by Experiment test tunnel, particularly the arrest of the slabbing process when a stable geometry is reached.

Failure criteria

In the *cohesive-brittle-frictional (CBF) model* yielding occurs when the constant deviatoric stress criterion for damage initiation (e.g. σ_1-σ_3 = $\sigma_c/3$) is exceeded, cohesion drops and friction is mobilized. Martin (1997) used laboratory values for residual cohesion and friction angle and the yield criterion σ_1-σ_3 = 70 MPa in the PHASES hybrid finite/boundary element program (Carvalho et al., 1991) to produce a distribution of yield points that resembled the microseismic locations. Although Martin (1997) failed to reproduce the shape of the notch, he concluded that the simple constant-deviatoric-stress criterion was the most promising approach to estimating the onset of damage and the depth of brittle failure around the tunnel.

The *Unified Mises-Schleicher & Drucker-Prager (MSDPu) failure criterion*, developed by Aubertin et al. (2000) and implemented in PHASES hybrid finite/boundary element program (Carvalho et al., 1991), describes the short-term failure strength as well as the damage initiation threshold of rocks and Rockmasses. It includes a continuity parameter that is linked to the state of damage in the media, which in turn reflects the porosity of the intact rock and the discontinuity characteristics in a Rockmass. Time and size effects are explicitly included in the formulation. The influence of time is described by an extension of the subcritical crack growth theory in which the damage initiation threshold is introduced, this threshold corresponding to the long-term rock strength. Size effects are treated using a generalized version of existing power-law expressions. The progressive development of the notch geometry in the Mine-by Experiment test tunnel was modelled, showing fair agreement with the observed size and time effects (Aubertin et al., 2000).

Damage models

Damage-driven models (i.e. models that gradually change the material characteristics as damage occurs) have also been applied to the Mine-by Experiment. Eberhardt et al. (1999) conducted a series of laboratory experiments on Lac-du-Bonnet granite to quantify the damage caused by uniaxial compression and its influence on rock deformation. It was found that Young's modulus, Poisson's ratio and acoustic emission properties are all functions of strain. Cai et al. (2001) developed a damage-driven modelling method that can accommodate both isotropic or anisotropic fracture distributions. Seismic data is used to derive the fracture distribution, with the source dimensions of microseismic events near underground openings estimated assuming a tensile rather than a shear mechanism. The calculated fracture density is used to degrade the Young's modulus and Poisson's ratio. Data from the Mine-by Experiment was used to validate the method. It was found that the damage-driven softening model gave a good match with the extensometer measurements of radial deformation.

A compressive failure test on Lac-du-Bonnet granite core sample was simulated using PFC^{2D} (Itasca, 1995b) by calculating the relationship between axial strain and the number and rate of tensile and shear cracks (Diedrichs, 1999, cited by Hajiabdolmajid et al., 2002). The PFC^{2D} code was

extended to simulate acoustic emissions during laboratory testing of rock samples by grouping bond-breakages that are close together in time and space to create microseismic events with a range of energies (Hazzard and Young, 2000; Chandler et al., 2002). The method was validated by comparison with a laboratory stress-strain and acoustic emission data. The algorithm succeeded in generating rock failure without the need to incorporate any constitutive macro failure criteria, and produced power-law frequency-magnitude distributions with b-values similar to those obtained in the laboratory. However, it did not succeed in modelling post-failure behaviour.

3 KEY ISSUES IN DATA-DRIVEN MODELLING

3.1 Description of Rock Properties

The intrinsic variability of rock properties may be incorporated into the numerical modelling scheme by means of a statistical distribution of rock properties. Changes in rock properties as the stress field evolves and the rock degrades may be incorporated by schemes to adjust parameters such as rock stiffness and strength. Examples are given by Fang and Harrison (2001, 2002a and 2002b); Tang (1997); Tang and Kaiser (1998); Kaiser and Tang (1998) and Tang et al. (2000a and 2000b).

Another vexed question is the relationship between the in situ and laboratory measured properties. Mohammed et al. (1997) reviewed several thousand papers on numerical modelling and found that only a few hundred mentioned laboratory and Rockmass properties, and of those, only some 44 appeared to apply some kind of reduction. They found that compressive strength, on average, was reduced to about a quarter of the laboratory value, and stiffness to about half. They caution that the modelled Rockmass property values are not necessarily measured or 'back analysis derived' and could be, in some cases, simply the opinion of the author of the paper and thus reinforce a bias towards conventional wisdom. They compared the fit of the equations that have been proposed to the data, and concluded that the following equation formulated by Mitri et al. (1994) appeared to give the best prediction to the stiffness properties, at least for RMRs above 20:

$$RF = \frac{E_{rm}}{E_{int}} = 0.5\left(1 - \left(cos\left(\pi \frac{RMR}{100}\right)\right)\right)$$

where RF is the reduction factor; E_{rm} and E_{int} are the Young's modulus of the Rockmass and intact rock, respectively; and RMR is the Rockmass rating.

In terms of strength properties, Mohammed et al. (1997) recommended the approach of Hoek and Brown (1980), which has subsequently been refined and extended (Hoek and Brown, 1997; Hoek, 1998).

$$\sigma'_1 = \sigma'_3 + \sigma'_3\left(m_b \frac{\sigma'_3}{\sigma_{ci}} + s\right)^a$$

where σ'_1 and σ'_3 are the maximum and minimum effective stresses at failure, respectively; m_b is the value of the Hoek-Brown constant m for the Rockmass; s and a are constants ~~which~~ depend on the characteristics of the Rockmass, and σ_{ci} is the uniaxial compressive strength of the intact rock pieces (for intact rock, s =1 and a = 0.5). Hoek and Brown (1997) recommend that the values of the m_i be determined by a statistical analysis of the results of a set of triaxial tests on carefully prepared core samples. When using the Hoek-Brown criterion to estimate the strength of jointed Rockmasses, the Geological Strength Index (GSI) is used to estimate the Rockmass parameters m_b, s and a:

$$m_b = m_i \exp\left(\frac{GSI - 100}{28}\right) \text{ and } s = \exp\left(\frac{GSI - 100}{9}\right)$$

For rocks of reasonable quality (GSI>25), a = 0.5.

3.2 Constitutive Equations and Failure Criteria

A stress-strain curve for a uniaxial compression test can be divided into four segments from the onset of loading until peak strength (UCS) is reached: (i) crack closure, (ii) elastic deformation, (iii) stable crack growth, and (iv) unstable cracking associated with permanent axial deformation. Only the second stage is strictly linear elastic. Stable cracking typically initiates at uniaxial loads between 0.3 and 0.5 UCS in low-porosity rocks. The stress at which unstable cracking commences is a good indication of the long-term strength of a rock. It is typically initiated between 0.7 and 0.8 UCS, where a reversal in slope of the volumetric strain curve indicates that the rock is experiencing macro-scale dilation (Martin, 1997). A useful technique to analyse the linearity of the stress-strain curve is to compute a moving point linear regression (Eberhart et al., 1998). See, for example, Figure 1b. The extent to which a linear relation approximates the other segments depends on the rock type. Nevertheless, when used with care and insight, linear elastic codes can give very useful results.

Numerous failure criteria have been proposed. Several reviews and comparisons have recently been published. Colmenares and Zoback (2002) examined seven different failure criteria by comparing them to published polyaxial ($\sigma_1>\sigma_2>\sigma_3$) test data for five different rock types (dolomite, sandstone, limestone, shale and amphibolite) at a variety a stress states. The polyaxial Modified Wiebols-Cook and Modified Lade criteria achieved a good fit to most of the test data, especially for those rocks with a highly σ_2-dependent behaviour. However, the failure of some rock types is scarcely affected by σ_2 and the Mohr-Coulomb and Hoek-Brown criteria fit the test data equally well, or even better, than the more complicated polyaxial criteria. In general, the Circumscribed and Inscribed Drucker-Prager failure criteria did not accurately indicate the value of σ_1 at failure.

3.3 Choice of Numerical Modelling Code

There are numerous factors to be considered when choosing a numerical modelling code, e.g. ease of data input, speed of computation, size and detail of model, nature of Rockmass (continuity, heterogeneity, etc.), geometry of the excavations, desired accuracy of solution. Most commonly used stress analysis codes used for mine design are based on either the boundary element or finite elements methods, each having merits and limitations. Boundary element codes are able to model complex mine geometries excavated in homogeneous and elastic rock very efficiently, but experience difficulty handling inhomogeneous Rockmasses. Finite element codes, on the other hand, easily incorporate inhomogeneities but require considerably more disk space and running time, thereby limiting the number of elements that can be used to construct a model. Ideally, the practitioner should have a range of codes available and sufficient insight to choose the code(s) and input parameters most suitable to the job at hand.

The discontinuous nature of the Rockmass is sometimes fundamental to the problem being addressed. For example, when simulating caving, blasting, fault-controlled deformation or the behaviour of highly fractured rock, treating the Rockmass as a continuum could lead to misleading conclusions. The basic difference between discrete element methods and continuum-based methods is that the contact patterns between components of the system are continuously changing with the deformation process for the former, but are fixed for the latter. This introduces a whole range of challenges, e.g. space sub-division and identification of

block system topology, representation of block deformation, algorithms for contact detection, constitutive equations for rock blocks and fractures (Jing, 2003).

4 CONTINUUM MODELLING

4.1 Rock[3D]FE

We decided to commence our study of numerical stress analysis codes by using Rock[3D]FE to model the 'room and pillar' model. Rock[3D]FE is a three-dimensional static finite element code that employs the simplest constitutive model, viz. linear-elastic. (Yu et al., 1996 and 1999; Li et al., 2002). It was developed by CANMET-MMSL to handle large-sized mine models. The pre- and post-processors were improved to aid data input and the interpretation of results, and the solution time was drastically reduced by restructuring the data handling procedures. A model consisting of 1 million elements can be run in 24 hours on a standard desktop computer. Analytical values that can be viewed include: σ_{xx}, σ_{yy}, σ_{zz}, τ_{xy}, τ_{yz}, τ_{xz}, σ_1, σ_2, σ_3, Hoek-Brown and Drucker-Prager failure criteria and the mining-induced Strain Energy density.

4.1.1 Merits and limitations

The most obvious limitation of the Rock[3D]FE code is the assumption that rock has linear elastic properties. The assumption of a linear stress-strain relationship is only reasonably valid between 40 and 80 MPa or 0.3 to 0.6 UCS (Figure 1a). A potential second limitation of Rock[3D]FE, in the case of this study, is that the code is unable to handle excavations at or near the model boundaries, so it is necessary to embed the volume for which solutions are required in a base volume that is at least 5-times larger. As large elements can be used to construct the base volume, the number of additional elements is not a serious issue. The problem arises from the fact that the physical model was bounded in space, with Teflon sheets minimizing friction between the block and the platens. So, although horizontal confinement is applied to the roof and the floor, the twin pillars carry the entire load applied to the top surface. In the case of the Rock[3D]FE model, however, some of the load applied to the boundary above the top surface of the block is not carried by the pillars, but is transferred through the abutments within the base volume. This effect was immediately apparent when the average pillar stress (APS) calculated by Rock[3D]FE was compared with the APS derived from tributary area theory. In order to reduce this effect, the pillar system was extended into the base volume.

4.1.2 Deformation and damage localisation

The deformation of the model was calculated using the laboratory-derived parameters (Table 1). Rock[3D]FE solves the stresses experienced by each brick element. An example output is shown in Figure 2. Strains are simply calculated using:

$$\varepsilon_{xx} = \frac{1}{E}\left[\sigma_{xx} - \upsilon(\sigma_{yy} + \sigma_{zz})\right]$$

and similarly for ε_y and ε_z.

The strain calculated by Rock[3D]FE is significantly smaller than the strain measured in Pillar 2, while negligible strain was measured on Pillar 1. With the benefit of the experimental observations, several factors were identified that contribute to this discrepancy: (i) non-linearity of Young's modulus E, (ii) asymmetrical loading of the pillars, and (iii) shear failure of Pillar 1. While it is possible to get a better match between the observed and calculated strains in Pillar 2 by reducing E, this does not correspond to physical reality and has no value in predicting the load at which failure will occur or where damage will be localized. In an attempt to simulate the shear failure of Pillar 1 and its incapacity to bear load, a 'single pillar' model was created by removing the pillars to the left of the line of symmetry. An APS of 116 MPa was calculated for Pillar 2. Because of the asymmetric loading, the strain on the 'inside' of Pillar 2 was 0.25 per cent, while the strain on the 'outside' was 0.18 per cent. While this gave a better match to the observed deformation, the specification of the fictitious model extending beyond the boundaries of the physical model into the base volume was rather arbitrary.

4.1.3 Localisation of failure

Several parameters calculated by Rock[3D]FE can be used as indicators of rock failure:

Peak compressive or tensile stresses (MPa): Failure may occur when the stress, compressive or tensile, exceeds the strength of the rock. Rock[3D]FE shows the presence of high compressive stresses at the corners of the excavation, precisely where the notches and fractures were observed to form. This parameter is simplistic, however, as it only considers a single component of the stress tensor and does not take the strengthening effect of confinement into account.

Strain Energy density (MJ/m³): Yu et al. (1996) suggest that this parameter can be used as an indicator of the rockburst hazard once a threshold has been established by calibration studies. This parameter considers all stress and displacement components into account to calculate the elastic energy stored in each brick element. In this instance, high values of strain energy density are coincident with high values of compressive stress.

Drucker-Prager failure criterion: The Drucker-Prager criterion, originally developed for soil mechanics, may be considered a generalization of the Mohr-Coulomb criterion as its parameters are related to the internal friction and cohesion of the material (Colmenares and Zoback, 2002). It is thus based on a shear failure concept. A 'circumscribed' Drucker-Prager criterion is implemented in Rock[3D]FE (i.e. an outer bound touching the outer apices of the Mohr-Coulomb hexagon, which predicts failure at higher stresses than the 'inscribed' criterion). Even at the load at which failure occurred (33.6 MPa), the factor of safety exceeds unity throughout the pillar (see Figure 2). However, the 'hourglass' geometry of the zone with a lower Safety Factor is apparent, indicating that spalling of the pillar walls could occur at higher loads.

Hoek-Brown empirical failure criterion: In the Rock[3D]FE implementation, the rock is considered likely to fail if the Safety Factor (SF) < 1, with:

$$SF = \frac{[s\sigma_c^2 + (-m\sigma_c\sigma_1)]^{1/2}}{[\sigma_1 - \sigma_3]}$$

where σ_1 and σ_3 are the major and minor principal stresses with compression negative and σ_c, m, s are the Hoek-Brown parameters. Using the laboratory derived Hoek-Brown parameters as initial values, it was found that the Safety Factor exceeded unity throughout the pillar. The 'single pillar' model subjected to the load at failure (33.6 MPa) was considered next. Again, the Safety Factor exceeded unity throughout the pillar. Sensitivity tests were carried out: decreasing s (to 0.5) and σ_c (to 100 MPa) led to predictions of failure on the inside of the pillar, similar to the observed spalling mode of failure in Pillar 2. Decreasing m (to say 5) did not have a significant effect.

It is desirable to have a rational basis for degrading the intact rock parameters. Our carved test blocks did not contain any joints; hence, it is not meaningful to use the GSI as a basis for altering m or s. A correction for size effect seems to be a

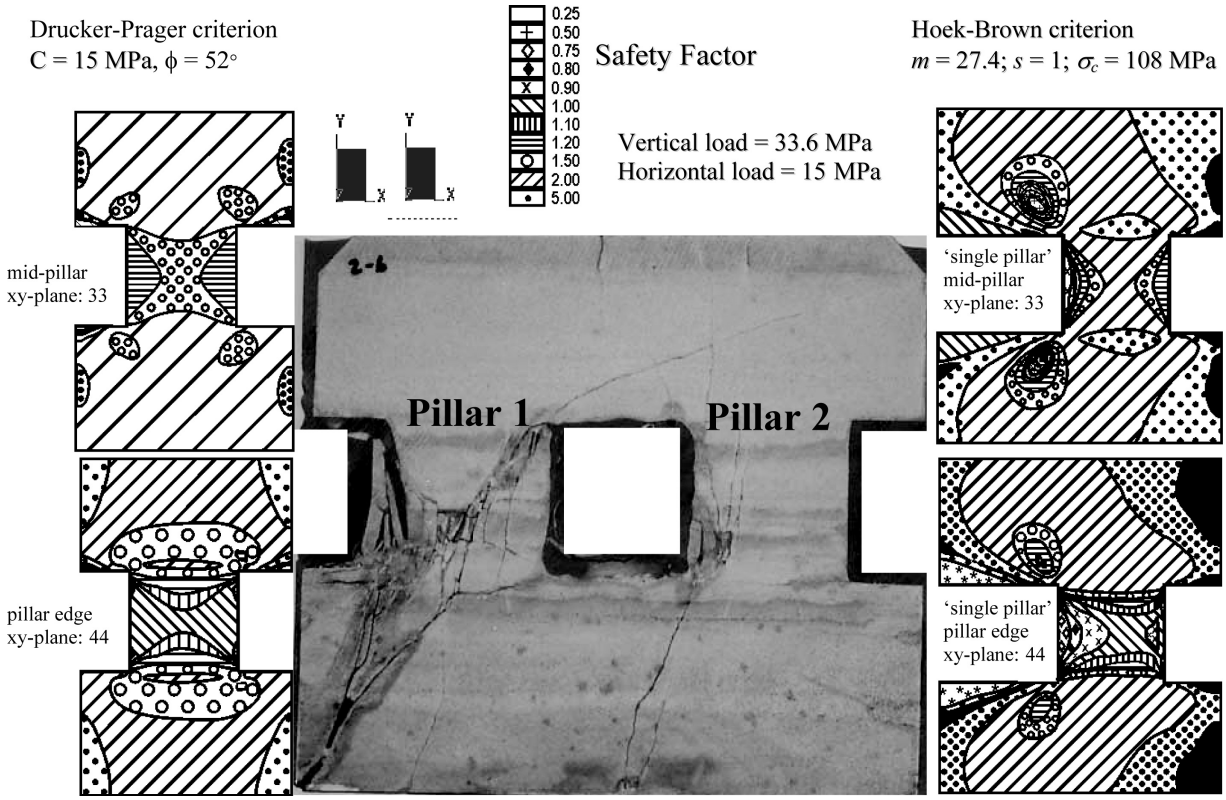

FIG. 2 **Rock[3D]FE modelling of the Block #2 'room and pillar' model. Drucker-Prager and Hoek-Brown failure criteria are compared with a slice through Block #2. Values less than unity indicate that rock failure is likely. The uniaxial compressive strength has been degraded to take the size of the block into account. The 'single pillar' model was used to calculate the Hoek-Brown Safety Factors**

better option. Hoek and Brown (1980) suggest the following relationship between the uniaxial compressive strength σ_{cd} of a rock specimen with a diameter of d mm, and the uniaxial compressive strength σ_{c50} of a 50 mm sample:

$$\sigma cd = \sigma c50\left(\frac{50}{d}\right)^{0.18}$$

Thus the uniaxial compressive strength of a specimen with a diameter of 250 mm, comparable in size to our carved blocks, would be expected to have a uniaxial compressive strength of 0.75 σ_{c50}. In the case of Block #2, the Hoek-Brown parameters were determined on cylindrical specimens with a diameter of 44 mm. Thus σ_{c44} = 147 MPa, translates to a σ_{c50} of 144 MPa and a σ_{c250} of 108 MPa. Using this value, the Hoek-Brown criterion indicated that failure was likely to occur (Figure 2).

4.1.4 Data-driven modelling

Several of the interventions described above exemplify the principles of 'data-driven' modelling:

Modification of the model. The elimination of Pillar 1 from the Rock[3D]FE model is an extreme form of 'the removal of failed elements' approach, but where the failed elements were identified based on the deformation measurements and damage observations, not on the output of the numerical model. The 'single pillar' model gave a better match to the observed deformation, the load at failure, and the localization of damage in Pillar 2. However, the specification of the fictitious model extending beyond the boundaries of the physical model into the base volume to comply with tributary area theory was rather arbitrary.

Reduction of rock properties determined in the laboratory. The reduction of the UCS used for the Hoek-Brown criterion was based on an empirical relationship describing the size effect (Hoek and Brown, 1980). In the field situation, the reduction of laboratory rock properties to those applicable to the in situ Rockmass should be based on geotechnical observations and sound empirical rules, for example, the measurement of the joint density and joint surface properties to calculate appropriate *m* and *s* parameters (Hoek and Brown, 1997).

While Rock[3D]FE is a powerful program, it could be enhanced by providing a greater range of failure criteria and heterogeneity into the model.

4.2 CANSAFE[3D]

4.2.1 Merits and limitations

CANSAFE[3D] (Li et al., 2003) is a finite element code that has several advantages over Rock[3D]FE (software not completed when used). Firstly, it can perform linear-elastic and elasto-plastic analyses using either the Drucker-Prager, Hoek-Brown or Van Mises failure criteria. Secondly, rock support and liner elements can be incorporated. Thirdly, it can handle the actual experimental boundary conditions. It is not necessary to create a fictitious 'base volume', unlike Rock[3D]FE. CANSAFE[3D] version 3.0 was used to simulate the "room and pillar" experiment.

4.2.2 Deformation

The results were in most respects similar to the outputs of Rock[3D]FE described above. The non-linear constitutive laws did not give any significant improvement in predicting the localization of damage or the load at failure.

5 DISCONTINUUM MODELLING

It is probable that the prominent shear fracture within Pillar 1 developed early in the test, and that Mohr-Coulomb type slip played an important role in the deformation and localization of damage. The displacement along the fracture was probably quite large, perhaps of the same order as the

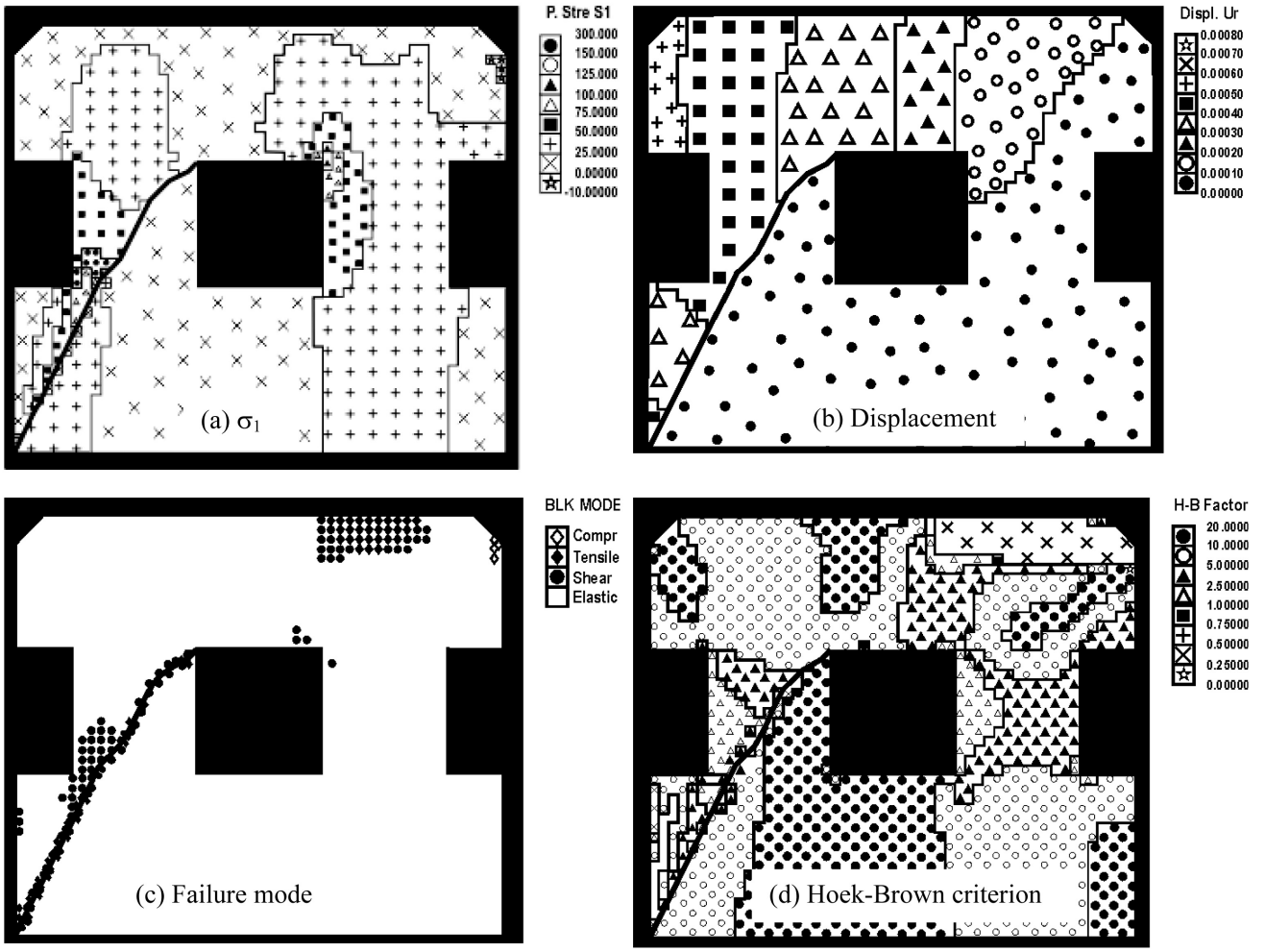

FIG. 3 **BSM^{3D} modeling of the 'room and pillar' model. Vertical load=23 MPa, Unilateral confinement=15 MPa, E=40 GPa, υ=0.3, UCS=108 MPa, C=15 MPa, ϕ=45°, m=27, s=1, K=100 MPa**

size of the elements used in continuum modelling. Hence, discontinuum rather than continuum modelling is more appropriate to the situation.

5.1 BSM^{3D} (Discrete Element Code)

BSM^{3D} (3-D Block-Spring Model) is a code developed by CANMET-MMSL researchers to simulate the behaviour of jointed Rockmasses (Wang and Garga, 1993; Wang et al., 1997; Li and Wang, 1998; Li and Vance, 1998; Li et al., 2002). The method is based on the assumption that a Rockmass can be represented by a system of isolated rigid blocks connected by springs in a state of equilibrium. Changes in the internal and external stress conditions cause the stress to be redistributed. The blocks are allowed to slide and detach along joint faces and soft layers in an iterative procedure until a new equilibrium state is achieved. For non-linear analysis, the Mohr-Coulomb failure criterion is used to examine failure conditions along the joints. If normal or shear-failure occurs, the driving force is replaced with a resisting force determined by the failure criterion and the blocks displaced until a new equilibrium state is achieved.

5.1.1 Merits and limitations

The output of BSM^{3D} is quite sensitive to mesh geometry. To investigate this, a rectangular mesh was generated. Loads of 34 MPa and 15 MPa were applied to the top and left hand boundaries of a 25x22 m^2 model, respectively. The maximum displacement was 15 mm. An inclined discontinuity was then introduced with the same properties as the joints within the Rockmass. The discontinuity divided the elements through which it passed into smaller triangles and polygons. The stresses calculated in these elements show some small variations from the background value of 34 MPa, but the calculated displacements are virtually indistinguishable from the discontinuity-free model. Then the inclined discontinuity was "softened" by assigning it a normal and shear stiffness of 100 MPa/m, giving rise to a maximum slip of 60 mm. The exercise was then repeated, but using an inclined mesh generated so that one of the joints in the Rockmass can be designated as the "soft" discontinuity. As a result, the element size and inclination of the element boundaries varied. The stress and displacement fields were then calculated. It was found that they differed significantly from the model with rectangular elements, the maximum displacement being almost three times greater.

5.1.2 Deformation and damage

Modelling of the "room and pillar" model with a single "soft" discontinuity intersecting a pillar at load of 23 MPa is shown in Figure 3. The transfer of stress from the pillar weakened by the discontinuity is clearly demonstrated. Zones where shear, tensile and compressive failure occurred are apparent.

The Hoek-Brown Safety Factor is meaningless in failed areas, but can be used to gain some insight into the likely location of future damage in areas that are still modelled as elastic.

6 CONCLUSIONS

The long-term objective of this project is to develop better strategies and tools to simulate the response of an overstressed Rockmass to mining by gathering appropriate rock property, deformation and damage data and using it as input for numerical modelling codes. This paper is essentially a progress report describing the first stage of this project: (i) the development of competence and techniques to monitor the deformation, degradation, stress transfer and failure of triaxially loaded carved rock models in the laboratory, and (ii) the testing of CANMET-MMSL numerical modelling codes. Several opportunities to improve the codes have been identified.

It is planned to expand the work considerably, working with CSIR and commercial codes, and testing ways to incorporate measured strain, convergence and acoustic emission data into the modelling process. For the next series of tests, we plan to study and compare the response of similar "room and pillar" models carved from Barre granite, Cairnside sandstone and Matagami sulphide ore. We also plan to introduce a couple of new models, e.g. a 'tabular stope' and a 'discontinuous Rockmass'. Once we have gained confidence in our approach, we intend to undertake in situ mine studies.

ACKNOWLEDGMENTS

The authors gratefully acknowledge the support given to this international collaborative research project by Dr Güner Gürtunca and Mr Roy Sage, at the time directors of CSIR Miningtek and CANMET Mining and Mineral Sciences Laboratories, respectively. The laboratory work was carried out at CANMET's Bells Corners Complex in Ottawa, where Ted Anderson, Blain Conlon, Ken Judge and Glenn Poirer provided outstanding technical support. Other CANMET researchers that contributed to the project are Jane Alcott, Dr Marc Betournay, Russell Boyle, Chantale Doucet, Dr Véronique Falmagne, Bernie Gorski, Dr Gary Li, Michel Plouffe and Dr Shahriar Talebi. The CSIR researchers that contributed are Drs Milton Kataka, Lindsay Linzer, Ewan Sellers and Steve Spottiswoode.

REFERENCES

Aubertin, M., Li, L. and Simon, R. (2000) A multiaxial stress criterion for short- and long-term strength of isotropic rock media. Int. J. Rock Mech. Min. Sci., 37: pp. 1169-93.

Brady, B.H.G. and Brown, E.T. (1985). Rock Mechanics for Underground Mining, George Allen & Unwin, London, 527 pp.

Briggs, D.J. and Vieler, J.D.S. (1984) Microfractures studies of quartzite in triaxial extension. Internal Research Report 12/84, Chamber of Mines Research Organisation (now CSIR: Miningtek).

Cai, M., Kaiser, P.K. and Martin, C.D. (2001) Quantification of Rockmass damage in underground excavations from microseismic event damage. Int. J. Rock Mech. Min. Sci. 38: pp. 1135-45.

Carvalho, J.L., Hoek, E. and Corku, B.T. (1991) PHASES – A 2D hybrid finite/boundary element program for calculating stresses and estimating support around underground openings, Version 2.0, User's Guide, Rock Engineering Group, Department of Civil Engineering, University of Toronto, Canada.

Chandler, N., Read, R., Potyondy, D., Young, R.P. and Hazzard, J. (2002). Computing brittle rock fracture and excavation stability using the particle flow code. In Proceedings of the 2nd Canadian Special Conference on Computer Applications in Geotechnique, The Canadian Geotechnical Society (CGS), Winnipeg (MN), pp. 104-111.

Colmenares, L.B. and Zoback, M.D. (2002) A statistical evaluation of intact rock failure criteria constrained by polyaxial test data for five different rocks. Int. J. Rock Mech. Min. Sci. 39: pp. 695-729.

Curran, J.H. and Corkum, B.T. (1995) Examine2D, A 2D boundary element program for calculating stresses around underground excavations in rock, Version 5.0, User's Guide, Rocscience Inc., Rock Engineering Group, Department of Civil Engineering, University of Toronto, Canada.

Diedrichs, M.S. (1999) Instability of hard rockmasses: The role of tensile damage and relaxation. PhD thesis, Department of Civil Engineering, University of Waterloo, Waterloo, Canada, 566 pp.

Durrheim, R.J. (2002) Stability and support of tunnels and orepasses in ultra-deep Witwatersrand gold mines: findings of the DEEPMINE Research Programme. In Proceedings of the 2nd International Seminar on Surface Support Liners, South African Institute of Mining and Metallurgy, section 10, 6 p.

Durrheim, R.J. and Labrie, D. (2004) Data–driven simulation of the Rockmass response to mining (Part 1): Laboratory experiments using Nepean sandstone models. In Proceedings of the 2nd International Seminar on Deep and High Stress Mining, SA Inst Min. Metall. Symposium Series.

Eberhardt, E., Stead D., Stimpson, B. and Read, R.S. (1998) Identifying crack initiation and propagation thresholds in brittle rock. Can. Geotech J. 35: pp. 222-33.

Eberhardt, E., Stead, D. and Stimpson, B. (1999) Quantifying progressive pre-peak brittle fracture damage in rock during uniaxial compression. Int. J. Rock Mech. Min. Sci. 36: pp. 361-80.

Fang, Z. and Harrison, J.P. (2001) A mechanical degradation index for rock. Int. J. Rock Mech. Min. Sci. 38: pp. 1193-99.

Fang, Z. and Harrison, J.P. (2002a) Development of a local degradation approach to the modelling of brittle fracture in heterogeneous rocks. Int. J. Rock Mech. Min. Sci. 39: pp. 443-57.

Fang, Z. and Harrison, J.P. (2002b) Application of a local degradation model to the analysis of brittle fracture of laboratory scale rock specimens under triaxial conditions. Int. J. Rock Mech. Min. Sci. 39: pp. 459-76.

Gay, N.C. (1976) Fracture growth around openings in large blocks of rock subjected to uniaxial and biaxial compression. Int. J. Rock Mech. Min. Sci. 13: pp. 231-43.

Hajiabdolmajid, V., Kaiser, P.K. and Martin, C.D. (2002) Modelling brittle failure of rock. Int. J. Rock Mech. Min. Sci. 39: pp. 731-41.

Hallbauer, D.K., Wagner, H. and Cook, N.G.W. (1973) Some observations concerning the microscopic and mechanical behaviour of quartzite specimens in stiff, triaxial compression tests. Int. J. Rock Mech. Min. Sci. 10: pp. 713-726.

Hazzard, J.F. and Young, P. (2000) Simulating acoustic emissions in bonded-particle models of rock. Int. J. Rock Mech. Min. Sci. 37: pp. 867-72.

Hoek, E. and Brown, E.T. (1980) Underground Excavations in Rock, Inst. Min. Metall., London, 527 p.

Hoek, E. and Brown, E.T. (1997) Practical estimates of Rockmass strength. Int. J. Rock Mech. Min. Sci. 34: pp. 1165-1186.

Hoek, E. (1998) Reliability of Hoek-Brown estimates of Rockmass properties and their impact on design. Int. J. Rock Mech. Min. Sci. 35: pp. 63-68.

Hoffmann, G., Sewjee, R. and Van Aswegen, G. (2001) First steps in the integration of numerical modelling and seismic monitoring. In Proceedings of the 5th Int. Symposium on Rockbursts and Seismicity in Mines, (ed. G.A. van Aswegen, R.J. Durrheim and D.W. Ortlepp), South African Institute of Mining and Metallurgy, pp. 397-404.

Itasca (1995a) FLAC – Fast Lagrangian Analysis of Continua, Version 3.3. Itasca Consulting Group Inc., Minneapolis, USA.

Itasca (1995b) PFC - Particle Flow Code, Version 1.0. Itasca Consulting Group Inc., Minneapolis, USA.

Jing, L. (2003) A review of techniques, advances and outstanding issues in numerical modelling for rock mechanics and rock engineering. Int. J. Rock Mech. Min. Sci. 40: pp. 283-353.

Kaiser, P.K. and Tang, C.A. (1998) Numerical simulation of cumulative damage and seismic energy release during brittle rock failure – Part II: Rib pillar collapse. Int. J. Rock Mech. Min. Sci. 35: pp. 123-34.

Labrie, D., Boyle, R., Anderson, T., Conlon, B. and Judge, K. (2002) Propriétés des roches et réponse du massif lors du minage sous contrainte modérée et élevée. 104th Annual Meeting of the Canadian Institute of Mining, Metallurgy and Petroleum (CIM), Vancouver (B.C.), 25 p.

Li, G., Boyle, R., Udd, J.E. and Toews, N. (2002). Application of BSM3D and Rock3D in simulation of mining sequences under complex geological conditions. In Proceedings of the 2nd Canadian Special Conference on Computer Applications in Geotechnique, The Canadian Geotechnical Society (CGS), Winnipeg (MN), pp. 142-149.

Li, G., Boyle, R. and Wong, A.A. (2003) CANSAFE – a Windows application package for non-linear stress analysis using the finite element method. CANMET Report MMSL 03-086 (TR), Natural Resources Canada.

Li, G. and Vance, J. (1998) A 3-D block-spring model for simulating the behaviour of jointed rocks. In Rock Mechanics for Industry, (eds. B. Amadei, R.L. Kranz, G.A. Scott and P.H. Smeallie), Balkema, Rotterdam, pp. 141-146.

Li, G. and Wang, B. (1998) Development of a 3-D block-spring model for jointed rocks. In Mechanics of Jointed and Faulted Rock, (ed. H.P. Rossmanith), Balkema, Rotterdam, pp. 305-309.

Malan, D.F. (1999) Implementation of a viscoplastic model in FLAC to investigate rate of mining problems, In FLAC and Numerical Modelling in Geomechanics, (ed. C. Detournay, and R. Hart), Balkema, Rotterdam, pp. 497-504.

Malan, D.F. (2002) Simulating the time-dependent behaviour of excavations in hard rock. Rock Mech. Rock Engng. 35: pp. 225-54.

Malan, D.F. and Napier, J.A.L. (1995) Computer modeling of granular material microfracturing. Tectonophysics 248: pp. 21-37.

Martin, C.D. (1997) Seventeenth Canadian Geotechnical Colloquium: The effect of cohesion loss and stress path on brittle rock strength. Can. Geotech. J. 34: pp. 698-725.

Martin, C.D., Read, R.S. and Martino, J.B. (1997) Observations of brittle failure around a circular test tunnel. Int. J. Rock Mech. Min. Sci. 34: pp. 1065-73.

Mitri, H.S., Edrissi, R. and Henning, J. (1994) Finite element modeling of cable-bolted stopes in hard rock underground mines. Presented at the SME Annual Meeting, Albuquerque, New Mexico, 14-17 February, 1994, Paper Number 94-116.

Mohammad, N., Reddish, D.J. and Stace, L.R. (1997) The relation between in situ and laboratory rock properties used in numerical modelling. Int. J. Rock Mech. Min. Sci. 34: pp. 289-297.

Napier, J.A.L. (1990) Modelling of fracturing near deep level gold mine excavations using a displacement discontinuity approach. In Proceedings of the 1st International Conference on the Mechanics of Jointed and Faulted Rocks, (ed. H-P Rossmanith), pp. 709-715.

Napier, J.A.L. and Malan, D.F. (1997) A viscoplastic discontinuum model of time-dependent fracture and seismicity effects in brittle rock. Int. J. Rock Mech. Min. Sci. 34: pp.1075-89.

Sellers, E., Kataka, M.O. and Linzer, L. (2003) Source parameters of acoustic emission sources and scaling with mining induced seismicity. J. Geophys. Res., 108, pp. ESE 7-1 – 7-16.

Sellers, E. and Scheele, F. (1996) Prediction of anisotropic damage in experiments simulating mining in Witwatersrand quartzite blocks. Int. J. Rock Mech. Min. Sci. 33: pp. 659-70.

Spottiswoode, S.M. (2001) Keynote address: Synthetic seismicity mimics observed seismicity in deep tabular mines. In Proceedings of the 5th Int. Symposium on Rockbursts and Seismicity in Mines, (eds. G.A. van Aswegen, R.J. Durrheim and D.W. Ortlepp), South African Institute of Mining and Metallurgy, pp. 371-378.

Spottiswoode, S.M., Napier, J.A.L. and Kataka, M. (2003) Seismology in the design of mine layouts. In Proceedings of the 30th Int. Conf. of Safety in Mines Research Institutes, South African Institute of Mining and Metallurgy.

Tang, C.A. (1997) Numerical simulation of progressive rock failure and associated seismicity. Int. J. Rock Mech. Min. Sci. 34: pp. 249-61.

Tang, C.A. and Kaiser, P.K. (1998) Numerical simulation of cumulative damage and seismic energy release during brittle rock failure – Part I: Fundamentals. Int. J. Rock Mech. Min. Sci. 35: pp. 113-21.

Tang, C.A., Liu, H., Lee, P.K.K., Tsui, Y. and Tham, L.G. (2000a) Numerical studies of the influence of microstructure on rock failure in uniaxial compression – Part 1: effect of heterogeneity. Int. J. Rock Mech. Min. Sci. 37: pp. 555-69.

Tang, C.A., Tham, L.G., Lee, P.K.K., Tsui, Y. and Liu, H. (2000b) Numerical studies of the influence of microstructure on rock failure in uniaxial compression – Part 2: constraint, slenderness and size effect. Int. J. Rock Mech. Min. Sci. 37: pp. 571-83.

Udd, J.E. (2002) Deep mining in Canada – the challenges and opportunities. In Proceedings of the 1st International Seminar on Deep and High Stress Mining, Australian Centre for Geomechanics, Perth Australia, Section 3, 22 p.

Wagner, H. (1989) Underground openings in overstressed rock. In Proceedings of the 6th Int. Rock Mechanics Congress, Balkema; Rotterdam, pp. 1443-1456.

Wang, B. and Garga, V.K. (1993) A numerical method for modeling large displacements of jointed rocks – Part 1: fundamentals. Can. Geotech. J. 30: pp. 96-108.

Wang, B., Vongpaisal, S., Dunne, K. and Pakalnis, R. (1997) Prediction and measurement of hangingwall movements of Detour Lake mine SLR stope. In Computer Methods and Advances in Geomechanics, Vol. 2, (ed. J. Yuan), Balkema, Rotterdam, pp. 1571-1575.

Yu, Y.S., Vongpaisal, S., Bétournay, M., Toews, N.A. and Boyle, R. (1999) ROCK3DFE: A one million element+ modelling technology for rapid mine design and planning. CIM Bulletin 92: pp. 37-39.

Yu, Y.S., Toews, N.A., Boyle, R. and Vongpaisal, S. (1996) Very large-scale 3D modelling of mine structures using the finite element technique. In Proceedings of the 2nd North American Rock Mechanics Symposium, (ed. M. Aubertin, F. Hassani and H. Mitri), Balkema, Rotterdam, pp. 1871-1878.